OXFORD

Nanofiber–microsphere (nano-micro) matrices for bone regenerative engineering: a convergence approach toward matrix design

Clarke Nelson,[1] Yusuf Khan[1,2,3] and Cato T. Laurencin[1,2,4,*]

[1]Raymond and Beverly Sackler Center for Biomedical, Biological, Physical and Engineering Sciences, Institute for Regenerative Engineering, University of Connecticut Health Center, Farmington, CT 06030, USA, [2]Department of Orthopaedic Surgery, University of Connecticut Health Center, Farmington, CT 06030, USA, [3]Department of Materials Science and Engineering, University of Connecticut, Storrs, CT 06269, USA, [4]Department of Chemical and Biomolecular Engineering, University of Connecticut, Storrs, CT 06269, USA

*Correspondence address: 263 Farmington Avenue, Farmington, CT 06030-3711, USA. Tel: +1-860-679-4086; Fax: +1-860-679-1553; E-mail: Laurencin@uchc.edu

Abstract

Bone is an essential organ for health and quality of life. Due to current shortfalls in therapy for bone tissue engineering, scientists have sought the application of synthetic materials as bone graft substitutes. As a composite organic/inorganic material with significant extra cellular matrix (ECM), one way to improve bone graft substitutes may be to engineer a synthetic matrix that is influenced by the physical appearance of natural ECM networks. In this work, the authors evaluate composite, hybrid scaffolds for bone tissue engineering based on composite ceramic/polymer microsphere scaffolds with synthetic ECM-mimetic networks in their pore spaces. Using thermally induced phase separation, nanoscale fibers were deposited in the pore spaces of structurally sound microsphere-based scaffold with a density proportionate to the initial polymer concentration. Porosimetry and mechanical testing indicated no significant changes in overall pore characteristics or mechanical integrity as a result of the fiber deposition process. These scaffolds displayed adequate mechanical integrity on the scale of human trabecular bone and supported the adhesion and proliferation of cultured mouse calvarial osteoblasts. Drawing from natural cues, these scaffolds may represent a new avenue forward for advanced bone tissue engineering scaffolds.

Keywords: nanobiomaterials; bioceramics; medical device; bone

Introduction

Bone is a complex organ with diverse physiological, physical and endocrine roles [1–4]. Although bone has its own inherent regenerative capacity, this ability may be overwhelmed in certain diseases or conditions including osteoporosis, trauma and neoplasia where significant amounts of tissue are lost [5]. Bone defects of a certain size, called critical sized defects, are known to prevent the body from regenerating bone in the damaged area, but there are other scenarios that also prevent the body from regenerating bone in simple fractures, called nonunions. The etiology of these fracture nonunions is not currently known but has been associated with a number of risk factors including obesity, smoking, diabetes and other conditions [6].

The current treatment provided for patients with insufficient supply of bone is to supplement with bone tissue from additional sources (bone grafts). The current gold standard treatment for bone grafts is to use bone that patient donates to themselves, called autograft bone. This autograft bone is highly effective because it contains osteogenic cells that can directly produce bone, osteoinductive growth factors and cues that can instruct the cell fate of osteoblast progenitors and an osteoconductive matrix that allows for improved host integration of the graft. Unfortunately, these bone grafts, frequently taken from the iliac crest, necessitate a secondary surgery with its corresponding morbidities [7]. Additionally, certain diseases or conditions may require either higher quantity or quality of bone than may already exist within the patient.

Because of the shortfalls in autograft bone, physicians have looked toward allograft bone, or bone donated from cadavers. Allograft bone has much less of a constraint on quantity, but it carries with it the risk of disease transmission, and as a result, allograft tissue is heavily treated before implantation in the patient [8]. From this processing, allograft bone loses many of the desirable osteogenic and osteoinductive characteristics. Perhaps unsurprisingly, these devitalized allografts do not integrate well into host bone, with a reported rate of 60% failing to adequately integrate into the surrounding host tissue at the 10-year post-implant time point [9].

One potential method to solve the problem of insufficient bone tissue is to engineer an autograft replacement from synthetic polymers. Synthetic polymers are of great interest to tissue engineers because they can be designed to incorporate whichever physical, chemical and biological characteristics are necessary for any particular clinical situation. Many synthetic polymers do not bind directly to surface receptors on cells, they have been shown to cause an increase in extra cellular matrix (ECM) production, which can then allow the cells to interact with synthetic surfaces in a more direct manner [10]. By modifying the three-dimensional (3D) structure of the template upon which bone progenitor secretes ECM proteins, scientists may be able to more effectively incite osteoblasts to construct a more clinically appropriate 3D matrix. Such tailor-made scaffolds may be able to utilize or enhance the bone's own inherent regenerative machinery to regenerate host bone tissue that has been lost. Combining advanced materials scaffolds with biological cues, chemical signals, tissue-specific cells and knowledge of developmental is the goal of regenerative engineering [11].

Although synthetic, sintered, composite microsphere scaffolds have been shown to have efficacy in the past *in vivo* for small defects, scaling up the scaffold to treat large critical sized defects in humans will present a number of problems with nutrient and waste exchange [12]. In order to guide cell growth and differentiation on the interior of the scaffold where nutrients supply is lower, the scaffold may need to provide a set of physical or chemical clues that ensure the survival and phenotypic progression of a cell that may otherwise expire in the absence of such cues. In this report, these sintered, composite, microsphere scaffolds are modified by creating intraporous, biomimetic, nanofibers. The intraporous poly(L-lactide) nanofibers described in the study may serve as a more architecturally complex 3D template for ECM protein deposition. The modified scaffolds may therefore be more capable of inducing material-guided behavioral changes which could potentially reduce the reliance on exogenously added biologics for osteoinductivity. The purpose of this study is to attempt to gain a better understanding of how intraporous nanofibers may be applied in the setting of the more clinically relevant polymer/ceramic composite microsphere scaffolds as an advanced bone graft substitute.

Materials and Methods

Scaffold fabrication
To fabricate 17% hydroxyapatite/poly(L-lactide) (HA/PLLA) microspheres, the procedure of Borden *et al.* [2] was modified. Briefly, high molecular weight PLLA (Purac, Netherlands) was purchased and dissolved in dichloromethane (DCM) (Fisher Scientific, Hampton, VT, USA); 17% by weight nanocrystalline HA/PLLA (Berkeley Biomaterials, Berkeley, CA, USA) was then suspended by agitation in DCM. The resulting suspension of HA and PLLA in DCM was then added drop-wise into a solution of polyvinyl alcohol (PVA) and stirred at a speed of 250 RPM. The DCM was then allowed to evaporate

overnight as the composite microspheres formed in the oil/water immersion. The composite microspheres were then vacuum filtered from the PVA solution, washed with distilled/deionized (DDI) water and lyophilized for 24 h to remove any excess solvent. Once dried, the microspheres were sorted according to size (300–355, 425–600 and 600–710 μm), placed in a stainless steel sintering mold and heated for 90 min to sinter adjacent microspheres at a temperature of 178°C (451 K). The resulting sintered, composite microspheres were used for control groups in this study. To precipitate PLLA nanofibers in the pore spaces, the thermally induced phase separation (TIPS) procedure of Ma and Zhang [13] was followed. Briefly, the sintered composite microspheres were submerged in a solution of 0.25% PLLA in *N,N*-dimethylformamide (DMF) at room temperature (298 K). The solution was then submerged in liquid nitrogen (78 K) for 5 min to allow thermal equilibrium between the liquid nitrogen and the polymer solution. Although the temperature of the PLLA solution was not directly measured, it was observed that after 60 s, the liquid nitrogen was no longer vigorously boiling in the liquid nitrogen crucible. After 5 min of submersion, no boiling of the liquid nitrogen was evident. The polymer solution was then removed from liquid nitrogen and submerged in deionized water for 3 days with a water change every day. These PLLA hybrid scaffolds were then placed in the freezer, lyophilized to remove all water and stored in a vacuum to create synthetic, PLLA-microsphere scaffolds. To fabricate collagen nanofibers in the pore spaces of the scaffold, a solution of 0.1% collagen (BD Biosciences) was created and gelled according to manufacturer's instructions. Briefly, 10 × phosphate buffered saline (PBS) (Gibco), 9.21% rat tail collagen (BD Biosciences) and sterile DI water were put on ice. The 9.21% collagen solution was diluted to a final concentration of 0.1% in a final solution of 1 × PBS using appropriate amounts of 10 × PBS and DI water. The 0.1% collagen solution was then gelled using an appropriate amount of 1 M NaOH solution (Sigma). The resulting collagen-microsphere scaffolds were then lyophilized and stored in a vacuum.

Scanning electron microscopy
In order to visualize the ability of TIPS to produce nanofibrous networks of three different densities, field emission scanning electron microscopy (FESEM) was used. The scaffolds were first sputter coated with gold/palladium using a hummer sputter coater (Anatech, Hayward, CA USA). The resulting scaffolds were then inserted into the FESEM (Strata™ 400 STEM DualBeam, FEI) and operated at an accelerating voltage of 10 kV and 12 μA.

Mechanical testing
To establish the effect of nanofiber production on the underlying mechanical integrity of the scaffolds, they were subjected to compressive testing using an Instron machine (Norwood, MA, USA). Cylindrical scaffolds (5 mm (diameter) × 10 mm (height)) of both control and hybrid scaffolds were subjected to compressive modulus testing. An $n = 3$ was used for each scaffold group, and the crosshead speed used was 5 mm/min. Load versus displacement data were collected, converted to stress versus strain and evaluated to determine the compressive modulus of the scaffolds.

Cell culture
MC3T3-E1 subclone 4 mouse calvarial pre-osteoblasts were obtained (ATCC® CRL-2593™). The cells were cultured in growth medium of alpha minimal essential medium (αMEM) (Gibco, Thermo Scientific), 10% fetal bovine serum (FBS) (Gibco) and 1% penicillin/streptomycin (Gibco), released with 0.25% trypsin

(Gibco), and counted using a hemacytometer prior to seeding onto scaffolds. For both the live/dead and DNA assay, 2×10^5 MC3T3 cells were seeded onto 0.25% 5 mm × 10 mm cylindrical scaffolds and allowed to adhere at 37°C for 1 h. Two milliliters of growth medium was then added to the scaffolds in a 24-well plate, submerging the entire scaffold and media was changed every 3 days.

Live/dead cell viability

After 7 days of culture, the scaffolds were split longitudinally and imaged on microscope glass with confocal microscopy (Confocor 2, Zeiss, Germany). A live/dead assay (Invitrogen, Carlsbad, CA, USA) was run to determine the viability of cells cultured on control and 1% hybrid scaffolds (425–600 µm in diameter).

DNA assay

To determine the ability of scaffolds to support the proliferation of cells over time, DNA was used as an indirect measure of cell population at 1, 3, 7, 14 and 21 day time points. To measure DNA content, the PicoGreen assay was used (Invitrogen); 2×10^5 MC3T3-E1 mouse calvarial pre-osteoblast cells were seeded onto 10 mm (H) × 5 mm (D) scaffolds and allowed to adhere for 1 h at 37°C in a 24-well plate. The wells were then filled with 2 ml of growth medium and cultured for 21 days in a humidified atmosphere at 37°C and 5% CO_2. The media were changed every 3 days. Four groups were examined: control (no nanofibers), 0.25% PLLA/DMF, 1% PLLA/DMF and 2% PLLA/DMF.

Porosimetry analysis

Porosimetry of the scaffolds was accomplished by means of mercury intrusion porosimetry using an Autopore IV mercury intrusion porosimeter (Micromeritics). The microsphere size used was 300--355 µm. Intrusion pressure and resulting volume change was recorded and converted to porosity and pore diameter distribution. After completion of testing, all toxic waste was disposed of properly according to institutional protocols.

Statistical analysis

For statistical analysis between two groups, a Student's *t*-test was used, with a $P < 0.05$ set as the point of criticality. For comparison between multiple groups, a two-way analysis of variance with Tukey's *post hoc* honestly significant difference (HSD) test was used to determine statistical significance.

Results and Discussion

Regenerative engineering is an extension of tissue engineering that bridges the fields of advanced materials, stem cells and developmental biology [14]. This work represents a new approach to combine multiple material characteristics together into a single scaffold to augment the natural regenerative processes in musculoskeletal tissues. In order to exploit these processes, the authors have sought to mimic both the structure and attributes of human bone. Specifically, mechanically sound constructs combining synthetic polymers, ceramics and ECM-mimetic fibers, into a single architecture have been formed. The polymers, while relatively inert on their own, degrade at a predictable rate. Reliable degradation kinetics are especially beneficial for controlled release of encapsulated factors or other payloads like the ceramic hydroxyapatite used in the work presented here. Consistent erosion of the polymer/ceramic blend is potentially beneficial because it prevents bulk release ions to the site of injury and allows steady
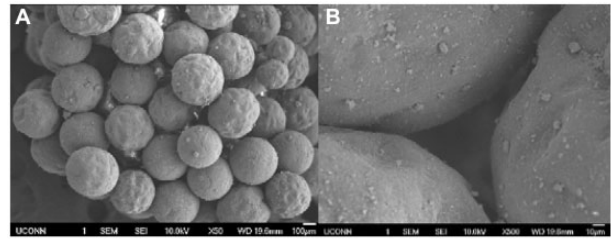

Figure 1. (A and B) 50× and 500× SEM view of sintered composite microsphere matrix. The pore spaces between microspheres form an interconnected pore network throughout the scaffold. Note in Fig. 1B a detail of the empty pore space.

release of osteoinductive calcium and phosphate [15]. Because they closely resemble natural collagen networks in bone, the ECM-mimetic fibers may have the potential to activate mesenchymal progenitor cells down the osteoblastic lineage. Furthermore, these intraporous nanofibers may augment the scaffold in two additional ways: these fibers may assist in the migration of cells throughout the scaffold and they may provide cells with additional surface area on which to lay down their own ECM. The second positive effect of providing additional surface area may be further expanded because osteoblasts are known to sense the underlying nanoscale features of their substrate and adjust their function accordingly [16]. Recently, Brown *et al.* [17] described a scaffold system that brought together sintered poly(phosphazene) microspheres and synthetic ECM-mimetic nanofibers. Although such 3D nanofibrous scaffolds have been studied extensively in a variety of contexts [13, 18–21], investigation of such nanofibrous technology in the pore spaces of the clinically relevant poly(alpha-hydroxy esters) family has not yet been published.

In order to determine whether these ECM-mimetic networks could be created in differing densities, three different concentrations of polymer solution were used to create the intraporous networks: 0.25%, 1% and 2% PLLA/DMF. As shown through SEM imagery in Figs 2–4, all three different concentrations of fibrous networks were fabricated successfully in the pore spaces of sintered microsphere scaffolds. In the low (50×) and high mag (500×) images of the control scaffold in Fig. 1, the pore space is adequately preserved throughout the sintering process, but is featureless and void. Comparing to the increasing concentrations of nanofibers pictured for 0.25%, 1% and 2% in Figs 2A–C, 3A–C and 4A–C, respectively, one can notice that these nanofibrous networks have a range of features across multiple size scales from 10 s of nanometers to hundreds of microns with a high degree of porosity (>90%). These attributes of the ECM-mimetic component are consistent with other observations in the field. In particular, as is visible in the 15 000× magnification images for each fiber concentration, there are multiple fibers which fall into the 50–500 nm diameter range, associated with natural collagen ECM networks in humans [21]. Features at this topographic level may potentially have the ability to exploit the natural physical cues that could drive cells toward the osteoblastic lineage [22–26]. In the 500× images, one can see that the fibers do not form a continuous network that occupies the entire pore space, but rather the fibers appear to form a sheet that bridges the pore space. The differences in morphology for this intraporous fibrous sheet at 500× are most noticeable between the 0.25% and both 1% and 2%. Differences between 1% and 2% are not striking at this magnification. All three concentrations look similar in both fiber diameter at the highest magnification (15 000×), and presence of 100 µm pores which may indicate that there is a lower limit to the amount of pore
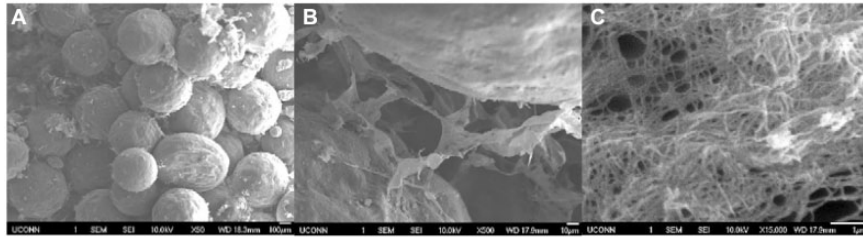
Figure 2. (A–C) 50× (left scale bar 100 µm), 500× (middle, scale bar 50 µm) and 15 000× (right, scale bar 1 µm) SEM of 0.25% nanofiber solution in a sintered composite microsphere matrix. On 500× magnification, the fibrous network is visible in the pore spaces between microspheres that was previously unoccupied by control scaffolds. A detailed view in Fig. 2C shows numerous fibers less than 500 nm in diameter.
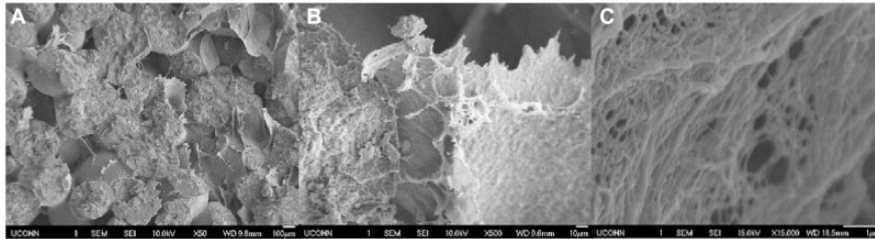

Figure 3. (A–C) 50× (left), 500× (middle) and 15 000× (right) views of 1% nanofiber solution. Notice the difference in lower scales to the 0.25% solution shown in Fig. 2B, but similarity to the lower concentration when viewed at high magnification (2C and 3C).
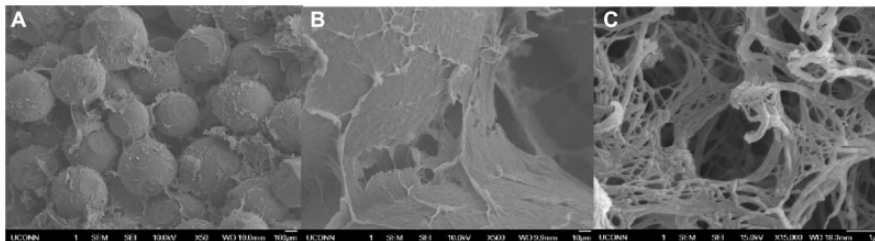

Figure 4. (A–C) 50× (left), 500× (middle) and 15 000× (right) views of 2% nanofiber solution. As with the comparison between 0.25% and 1%, there appear to be differences in pore size on larger scales (10–100 µm), but not on smaller scales (10–100 µm).

space that the nanofibers can occupy. One potential confounding factor for intraporous fiber morphology is the nature of the sample preparation for SEM. In order to examine the interior of the scaffold, the scaffolds have to be broken open. Such a mechanical manipulation is likely to damage the structure of these fibrous networks, but such manipulation would be very difficult to avoid. Other investigators have looked at the morphology of these intraporous fibrous networks in scaffolds formed through the use of porogens [20]. Examination of scaffolds in this manner allows less mechanical interruption of the intraporous elements, and in those reported cases, the fibrous networks did appear to bridge the entire pore space [20]. In the future, new scanning techniques will be investigated that may preclude the need for these scaffolds to be mechanically disturbed. Although on preliminary investigation, there did not appear to be any difference in fiber diameter at 15 000×, future techniques may develop that can allow more direct quantification of fiber diameters in the sub-micron range.

Due to the fact that the underlying sintered composite microsphere matrix for these scaffolds was exposed to weak PLLA solvent DMF, another concern was that the TIPS process may damage the underlying mechanical integrity of the scaffolds. The mechanical testing displayed in Table 1 showed that across all microsphere sizes and concentrations of nanofiber solutions, there was no statistical difference between groups. Additionally, all groups maintained

mechanical integrity on par with the lower end of human trabecular bone (100 MPa) [27]. Of note, the mechanical data for some scaffold groups displayed high variability. This level of variability did not change when separate experiments were attempted with higher numbers of scaffolds evaluated ($n = 6$ compared with $n = 3$) or tested using a different mechanical testing device (Bose ELF 3200). The high degree of variability is likely due to both the random nature of the bonds between adjacent microspheres during the sintering process and the polymer used to make the microspheres: a high molecular weight PLLA. This type of polymer is less amorphous and more crystalline than low molecular weight PLLA or poly(lactide-*co*-glycolide) (PLGA) formulations that have an observed glass transition temperature. The semi-crystalline PLLA has no such established glass transition temperature, and thus is in fact melting when forming adjacent bonds between microspheres. It is the experience of this research group that this process leads to a much higher degree of variability than sintering of PLGA microspheres. Taken together, these data indicate that this process for nanofiber formation in the context of a sintered microsphere scaffold would maintain its utility in a load bearing defect for bone repair.

Due to the DMF exposure, maintenance of porosity was also a concern. The porosity of all TIPS preparations was tested using a mercury intrusion porosimeter with a microsphere size of 300–355 µm. The smaller size of microspheres was assayed because it is

Table 1. Compressive modulus and compressive strength testing of scaffolds

Microsphere size (μm)	Polymer concentration	Compressive modulus (MPa)	Compressive strength (MPa)
300–355	Control	178 ± 2	14 ± 1.9
	0.25%	147 ± 11	9.3 ± 0.1
	1%	160 ± 44	14 ± 0.8
	2%	109 ± 12	6.2 ± 2.0
425–600	Control	170 ± 58	3.7 ± 0.9
	0.25%	105 ± 39	12 ± 2.2
	1%	317 ± 103	11 ± 3.0
	2%	202 ± 25	9.7 ± 0.8
600–710	Control	281 ± 107	12 ± 3.9
	0.25%	242 ± 36	5.9 ± 1.7
	1%	258 ± 51	4.4 ± 1.2
	2%	223 ± 34	8.9 ± 2.4

All units are in MPa. All errors displayed are standard errors of the mean. Across three different sizes of microspheres (300–355, 425–600 and 600–710 μm), and four different nanofiber concentrations (0%, 0.25%, 1% and 2%), no statistical difference was found through two-way ANOVA ($n = 3$) for evaluation of compressive modulus. The high variability of individual scaffold groups is likely due to the random nature of the sintering process.

Table 2. Results of mercury intrusion porosimetry testing

Polymer concentration	Percent porosity
Control	23 ± 9
0.25%	62 ± 5
1%	49 ± 2
2%	49 ± 2

Three scaffolds were used per group. Porosimetry shows hybrid scaffolds maintained high porosity after nanofiber precipitation procedure. Maintaining high porosity has been shown to be critical in nutrient and waste exchange.

known that decreasing the size of microspheres will have no effect on overall porosity, but it will have an effect on the number of large scale (>100 μm) pores [28,29]. It was found that all of the hybrid scaffolds types maintained a porosity of at least 40% porosity (shown in Table 2). Additionally, the scaffolds maintained evidence of larger pore spaces (~100 μm in diameter) that has been shown to help with mineralization of bone potentially due to maintenance of adequate nutrient and waste exchange (representative images shown below in Fig. 5A and B) [30]. These results, however, may be misleading because during the mercury intrusion process, it may be possible for the force of mercury to damage or destroy intraporous elements, and thereby artificially inflate the number of large pores present. Future studies will investigate further objective ways to quantify porosity that may not damage these intraporous environments.

To test the effect of nanofibers in the pore spaces of these scaffolds, MC3T3-E1 mouse calvarial pre-osteoblast cells were seeded onto both control and 1% hybrid scaffolds (425–600 μm in diameter) and cultured for 7 days in growth medium, and the cells were imaged under confocal microscopy with a live/dead assay to determine cell viability. The behavior of the MC3T3-E1 cell (subclone 4) is well-documented and highly predictable, and is a good choice when clarifying the effect of structural modifications on cell behavior, making them an ideal candidate to start initial *in vitro* tests. Primary cultures are less predictable given their inherent heterogeneity which, while more clinically relevant, may obscure the direct effect structural changes would have on cell behavior. The live/dead assay was used because the intracellular esterase activity of the green calcein-AM stain would permit not only the morphology of adherent cells to be investigated, but also whether the cell membranes were intact. The control scaffolds visualized were only able to support osteoblast adhesion on the surface of the microspheres, shown in Fig. 6A. Having cell viability limited to the periphery of microspheres in such a setting is potentially a limiting attribute of the scaffold for tissue engineering, especially when considering the physically larger structures that would be used in a clinical setting (vs. laboratory bone defect models). The hybrid nanofibrous
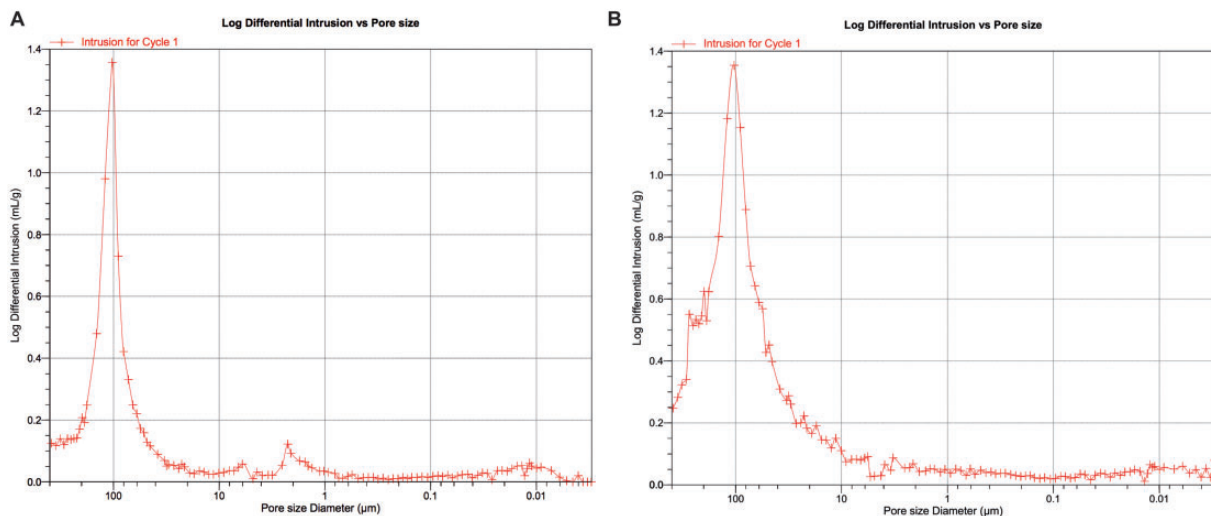

Figure 5. (A and B) Representative images of control scaffold with no nanofibers (A-left) and 0.25% hybrid scaffold (B-right). Although differences are notable between the control and hybrid nanofiber preparations, most importantly both scaffolds maintain a pore distribution that includes abundant pores around 100 μm in diameter. It is believed that this is the lower limit of pores that are conducive to bone tissue formation. Color version of this figure is available at http://rb.oxfordjournals.org/ online.
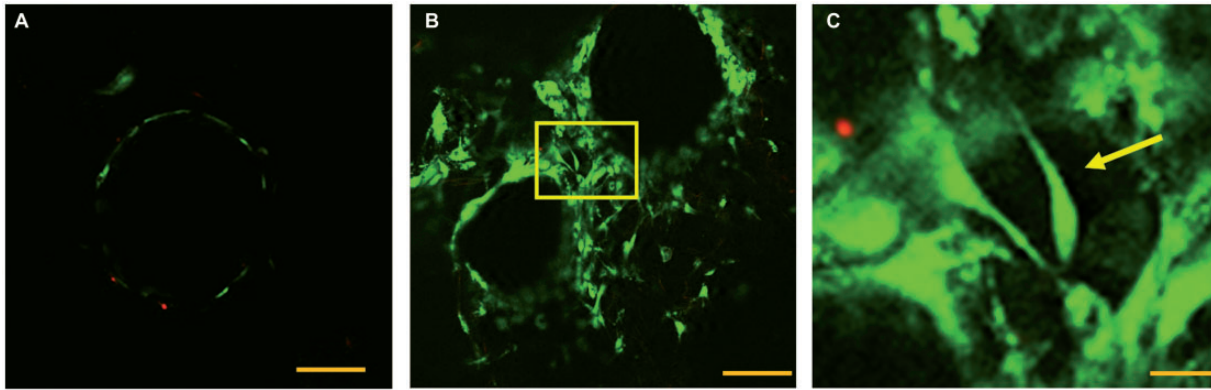
Figure 6. (A–C) Live/dead assay at 7 days. 2×10^5 cells were seeded onto control and 1% scaffolds (425–600 μm in diameter) and cultured for 7 days in growth medium to determine whether cells could adhere only to nanofibers alone. (A-left) The controls scaffolds, viable cells shown in green adhere solely to the surface of the microspheres (scale bar 100 μm). (B-middle) The pore space of a nanofiber-permeated pore space in a sintered microsphere scaffold. Cells appear to adhere not only to the surface of the microspheres but also to nanofibers. The detail of the pore space shown in C is indicated with a yellow box (scale bar 100 μm). (C-right) The detail of the pore space of a hybrid scaffolds showing a viable cell on nanofibers indicated with a yellow arrow (scale bar 10 μm). Color version of this figure is available at http://rb.oxfordjournals.org/ online.
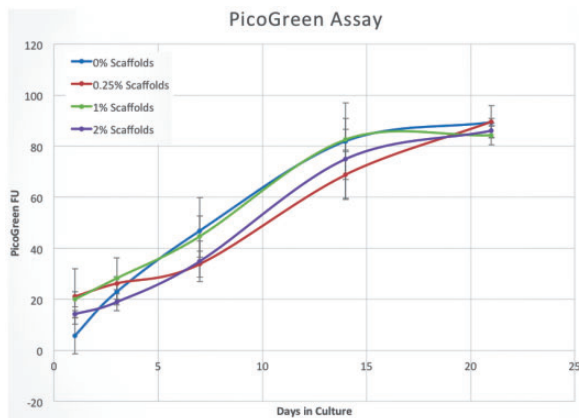

Figure 7. DNA content assay; 2×10^5 MC3T3 cells were seeded onto scaffolds and cultured for 21 days in growth medium. At 1, 3, 7, 14 and 21 day time points, the scaffolds were evaluated for DNA content. Although these data showed that the indirect marker for cell proliferation, DNA, increased from day 1 to day 21, there were no statistical differences in proliferation between groups. These results indicate that the presence of nanofibers in the pore spaces of the scaffold do not inhibit the underlying proliferative capacity of cells seeded on the sintered microsphere matrix. Color version of this figure is available at http://rb.oxfordjournals.org/ online.

scaffolds shown in Fig. 6B were able to support cell adhesion in their pore spaces as well as the surfaces of the microspheres. This may potentially be an improvement over the control scaffold architecture because additional surface area may allow additional space for cells to grow and higher populations of cells to be viable on these scaffolds. Figure 6C shows a detail of the pore space from Fig. 6B, and a cell appears to be adhering to the fibers alone and not in any direct contact with the surface of adjacent microspheres. This is a significant finding because it can indicate that the cells are not limited to contact with the microspheres for viability, thus potentially indicating that the entire pore volume could be accessible for adhesion and not simply the surface of the microspheres.

After looking qualitatively at cell adhesion, the next attribute tested on the scaffolds was DNA content as an indirect measure of cell proliferation. One lingering question about these nanofibrous networks is that while the addition of an appropriately dense nanofiber mesh to the pore spaces may facilitate cellular residence by providing more surface area for attachment and migration, too dense a fiber mesh may prohibit the migration of cells into the interior of the scaffold because the fibers may act as a mechanical barrier that is not porous enough to allow for the passage of cells. This would potentially abolish one of the desirable characteristics of the sintered microsphere scaffold engendered by its interconnected pore space: osteoconductivity, or the ability to allow the ingress of cells to the interior of the scaffold. As shown in Fig. 7, the ability of the underlying sintered, composite microspheres to support pre-osteoblasts was not affected by the additional of the nanofibrous pore element as measured through DNA content. Although this is not a strict test for osteoconductivity because the degree of migration cannot be measured in this manner, the live/dead assay supports the notion that cells are able to enter the interior of the scaffold. Together with SEM data from Figs 2–4 that showed a significant macropore (>100 μm) to the scaffolds, these data support the conclusion that the intraporous nanofibers do not act as a barrier to prevent entrance of cells migrating toward the interior of the scaffold, and the appropriate concentration of fibers may indeed facilitate greater cellular residence.

Conclusions

In this report, the authors have demonstrated a fabrication procedure for a novel scaffold combining ceramic and ECM-mimetic components for bone tissue engineering. These scaffolds do not suffer from reduced mechanical integrity, decreased macropore volume or ability to allow proliferation of a population of mouse calvarial pre-osteoblasts. The hybrid scaffolds discussed in this work will be used as a platform to evaluate more advanced regenerative engineering approaches *in vivo* including assessment of their incorporation with an appropriate population of stem cells or biological cues derived from understanding of developmental biology.

Funding

Acknowledgements

References

1. Lee NK, Sowa H, Hinoi E *et al*. Endocrine regulation of energy metabolism by the skeleton. *Cell* 2007;**130**:456–69.

2. Borden M, Attawia M, Khan Y *et al*. Tissue engineered microsphere-based matrices for bone repair: design and evaluation. *Biomaterials* 2002;**23**:551–9.

3. Calori GM, Mazza E, Colombo M *et al*. The use of bone-graft substitutes in large bone defects: any specific needs? *Injury* 2011;**42**(Suppl. 2):S56–63.

4. Colnot C, Zhang X, Tate ML. Current insights on the regenerative potential of the periosteum: molecular, cellular, and endogenous engineering approaches. *J Orthop Res* 2012;**30**:1869–78.

5. Kolk A, Handschel J, Drescher W *et al*. Current trends and future perspectives of bone substitute materials—from space holders to innovative biomaterials. *J Craniomaxillofac Surg* 2012;**40**:706–18.

6. Giannotti S, Bottai V, Dell'osso G *et al*. Current medical treatment strategies concerning fracture healing. *Clin Cases Miner Bone Metab* 2013;**10**:116–20.

7. Arner JW, Santrock RD. A historical review of common bone graft materials in foot and ankle surgery. *Foot Ankle Spec* 2014;**7**:143–51.

8. Ng VY. Risk of disease transmission with bone allograft. *Orthopedics* 2012;**35**:679–81.

9. Wheeler DL, Enneking WF. Allograft bone decreases in strength in vivo over time. *Clin Orthop Relat Res* 2005(435):36–42.

10. El-Amin SF, Lu HH, Khan Y *et al*. Extracellular matrix production by human osteoblasts cultured on biodegradable polymers applicable for tissue engineering. *Biomaterials* 2003;**24**:1213–21.

11. Lo KW, Kan HM, Gagnon KA *et al*. One-day treatment of small molecule 8-bromo-cyclic AMP analogue induces cell-based VEGF production for in vitro angiogenesis and osteoblastic differentiation. *J Tissue Eng Regen Med* 2013. doi: 10.1002/term.1839.

12. Khan Y, El-Amin SF, Laurencin CT. In vitro and in vivo evaluation of a novel polymer-ceramic composite scaffold for bone tissue engineering. *Conf Proc IEEE Eng Med Biol Soc* 2006;**1**:529–30.

13. Ma PX, Zhang R. Synthetic nano-scale fibrous extracellular matrix. *J Biomed Mater Res* 1999;**46**:60–72.

14. Laurencin CT, Khan Y. Regenerative engineering. *Sci Transl Med* 2012;**4**:160ed9.

15. Khan YM, Katti DS, Laurencin CT. Novel polymer-synthesized ceramic composite-based system for bone repair: an in vitro evaluation. *J Biomed Mater Res A* 2004;**69**:728–37.

16. Weng L, Webster TJ. Nanostructured magnesium has fewer detrimental effects on osteoblast function. *Int J Nanomedicine* 2013;**8**:1773–81.

17. Brown JL, Peach MS, Nair LS *et al*. Composite scaffolds: bridging nanofiber and microsphere architectures to improve bioactivity of mechanically competent constructs. *J Biomed Mater Res A* 2010;**95**:1150–8.

18. Feng G, Jin X, Hu J *et al*. Effects of hypoxias and scaffold architecture on rabbit mesenchymal stem cell differentiation towards a nucleus pulposus-like phenotype. *Biomaterials* 2011;**32**:8182–9.

19. Hu J, Ma PX. Nano-fibrous tissue engineering scaffolds capable of growth factor delivery. *Pharm Res* 2011;**28**:1273–81.

20. Wei G, Ma PX. Macroporous and nanofibrous polymer scaffolds and polymer/bone-like apatite composite scaffolds generated by sugar spheres. *J Biomed Mater Res A* 2006;**78**:306–15.

21. Wei G, Ma PX. Partially nanofibrous architecture of 3D tissue engineering scaffolds. *Biomaterials* 2009;**30**:6426–34.

22. Behring J, Junker R, Walboomers XF *et al*. Toward guided tissue and bone regeneration: morphology, attachment, proliferation, and migration of cells cultured on collagen barrier membranes. A systematic review. *Odontology* 2008;**96**:1–11.

23. Lamers E, te Riet J, Domanski M *et al*. Dynamic cell adhesion and migration on nanoscale grooved substrates. *Eur Cell Mater* 2012;**23**:182–93; discussion 193–4.

24. Muschler GF, Negami S, Hyodo A *et al*. Evaluation of collagen ceramic composite graft materials in a spinal fusion model. *Clin Orthop Relat Res* 1996(328):250–60.

25. Sverzut AT, Crippa GE, Morra M *et al*. Effects of type I collagen coating on titanium osseointegration: histomorphometric, cellular and molecular analyses. *Biomed Mater* 2012;**7**:035007.

26. Takeuchi Y, Nakayama K, Matsumoto T. Differentiation and cell surface expression of transforming growth factor-beta receptors are regulated by interaction with matrix collagen in murine osteoblastic cells. *J Biol Chem* 1996;**271**:3938–44.

27. Athanasiou KA, Zhu C, Lanctot DR *et al*. Fundamentals of biomechanics in tissue engineering of bone. *Tissue Eng* 2000;**6**:361–81.

28. Amini AR, Adams DJ, Laurencin CT *et al*. Optimally porous and biomechanically compatible scaffolds for large-area bone regeneration. *Tissue Eng Part A* 2012;**18**:1376–88.

29. Brown JL, Nair LS, Laurencin CT. Solvent/non-solvent sintering: a novel route to create porous microsphere scaffolds for tissue regeneration. *J Biomed Mater Res B Appl Biomater* 2008;**86**:396–406.

30. Hulbert S, Young F, Mathews R *et al*. Potential of ceramic materials as permanently implantable skeletal prostheses. *J Biomed Mater Res* 1970;**4**:433–56.